Grand Valley State University

ScholarWorks@GVSU

2009

Water Evaporation From Atmospheric Aerosols

Patrick Louden
Grand Valley State University

Christopher Lawrence
Grand Valley State University, lawrechi@gvsu.edu

Follow this and additional works at: https://scholarworks.gvsu.edu/sss

Part of the Chemistry Commons

Abstract

With the recent discovery of the ubiquity of organic material in tropospheric aerosols, it has been postulated that the rates of water evaporation and condensation into the aerosols could be affected by thin surfactant films, which could ultimately affect cloud formation. Nathanson *et al.* have begun to study the effect of water evaporation from sulfuric acid solutions through the short-chain surfactant, butanol. They have found that a nearly full monolayer of butanol fails to reduce water evaporation from the acid. This unexpected result raises many questions about the mechanism of water evaporation. We used molecular modeling to help answer some of these questions as it allowed us to examine the trajectory by which a molecule leaves the liquid at the molecular level. We also are able to study this problem under conditions closer to that of the troposphere because we are free of certain experimental limitations and we intend to do so in the future.

Introduction

Aerosols are tiny droplets of liquid suspended in air. Often times, aerosols will have other impurities within them or on them. The lowest layer of the atmosphere is called the troposphere. The troposphere is the layer in which the weather occurs. Aerosols that are composed of water are a key component in the formation of clouds and are necessary in radiation reflection. [1-7] With the recent discovery of organic molecules in the troposphere, experimentation was done to determine how the impurities may change the characteristics of the aerosols. The impurities that have been found in these aerosols encompass many different types of molecules. Differences in the nature of these molecules impact how they will behave within the aerosol. A molecule with a polar head and non-polar tail will stay on the surface of the aerosol whereas a salt will dissolve

and dissociate into its ionic parts within the liquid of the aerosol. [8-11] LaMer *et al.* studied water evaporation from pools of water with a covering of long carbon chained molecules. These carbon chains were between twelve and eighteen atoms in length, with a polar head. He determined that with a full coverage of surfactant, the rate of evaporation from the aerosol decreased by a factor of about 10,000. [12-13] Anticipating that longer chain surfactant molecules would not be present in the atmosphere due to photodegradation, Nathanson *et al.* studied evaporation through a surfactant of shorter carbon chains, using vacuum and mass spectrometry techniques. He studied the evaporation rate of an aerosol with a full coverage of butanol, a four carbon length molecule with a polar head. Due to the nature of his experiment, he used a system of supercooled sulfuric acid instead of that of water. This was done to keep the evaporation rate of the water very low creating a low vapor pressure above the system of interest allowing for precise measurements of how many molecules were evaporating. Nathanson found that with a full coverage of butanol, the evaporation rate of the aerosol was the same as a system with no butanol coverage. [14] By means of molecular modeling, we are looking at why there is no change in the evaporation rate between the two systems of supercooled sulfuric acid.

To begin to understand why this was occurring, Lawrence and Gilde first set up a model that consisted of water and butanol. Running the simulation for one nanosecond takes about one day computing time. In this nanosecond, they observed about zero evaporations occur. Since they needed a statistically meaningful number of several hundred instances of evaporation in order to calculate a rate, they had to run the simulation another way.

Since at equilibrium, the rate of evaporation is equal to the rate of condensation, they were able to measure the rate of condensation instead, which they were able to do in a much more computationally efficient manner. To do so, they introduced a water molecule in the gas

phase with a random displacement from the surface of the interface and a random velocity and allow it to strike the interface. [15] Upon collision with the surface, they anticipated three possibilities; condensation, inelastic scattering, and adsorption. Inelastic scattering occurs when a molecule collides with the surface of the interface and leaves without spending any significant amount of time at the interface; whereas an adsorption is a collision with the interface in which the gas phase molecule stays at the surface for an amount of time before finally escaping into the gas phase. After running 250 simulations, they obtained the percentages in Table 1. [16]

Table 1: The Percent of Condensation, Inelastic Scatter, and Adsorption With Respect to the Number of Butanol Molecules at the Interface

Butanol	Condense	Inelastic Scatter	Adsorption
0	100	0	0
8	91	2	7
18	83	6	11
32	60	24	16
50	33	38	28
72	37	43	20
98	52	31	17

Looking at Table 1, as expected the more butanol molecules that are on the interface the fewer molecules condense. This remains true until there are 72 butanol molecules on the interface when they saw that the number of condensations began rising again. This trend remains true at the 98 butanol coverage and poses the question of why this occurs. Looking at the columns for scatter and adsorption, the more butanol that are placed on the interface the greater the number of molecules are seen that either scatter or adsorb until a peak. The peak for

scattering occurs at the 72 butanol molecule coverage, and the adsorption peaks at 50 butanol molecules. For the rest of this discussion we will focus on the condensation percentages because through them, we will analogously be looking at the evaporation percentages of the system.

To understand why at the 72 and 98 butanol coverages the number of condensations increases, Lawrence and Gilde looked at how the butanol molecules are laying on the interface. By subtracting the position of the tail from the position of the polar head, they obtained a value for the height of the butanol. Figure 1 is a graph of the heights of the butanol for each level of interface coverage.

Figure 1: The Probability of Butanol Heights of Varying Interfaces
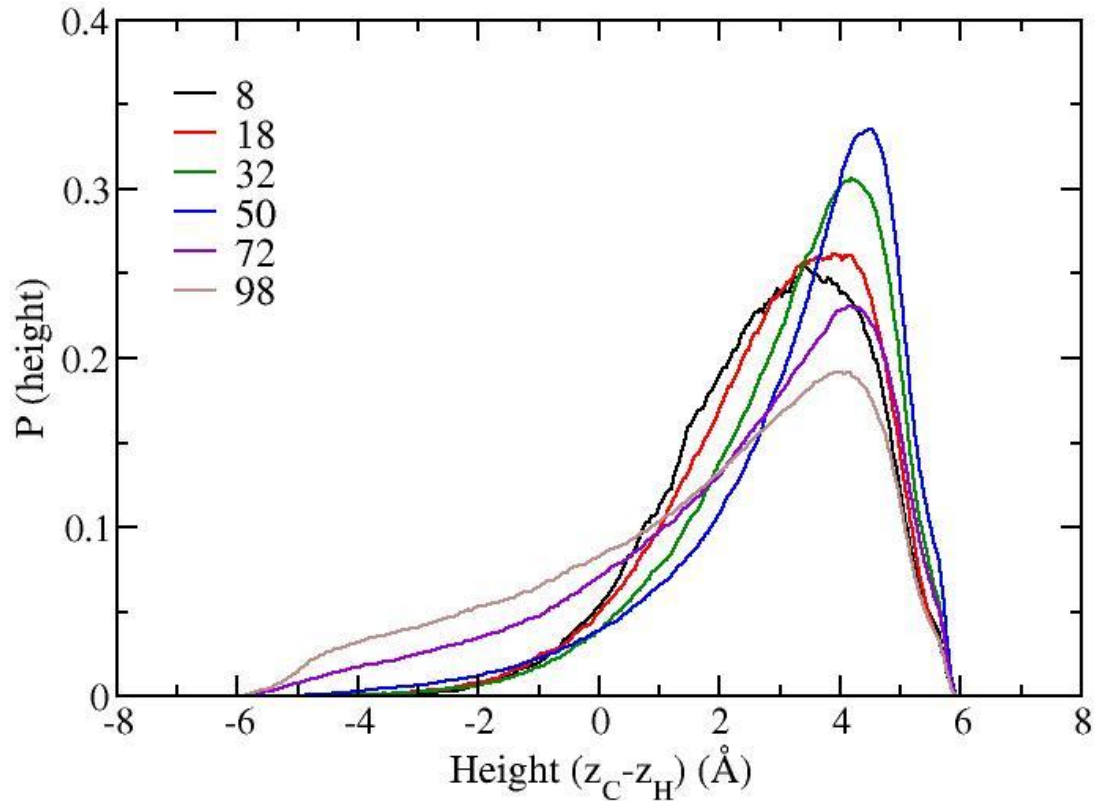
As seen in Figure 1, at low coverages of butanol, the height of the butanol is

short, as seen in Figure 1, for butanol molecule coverages 8-32. If there is an increase in the

number of butanol on the interface, there is an increase in the height of the butanol. This tells us

the more butanol molecules that are placed onto the interface the closer they are placed to one

another and the straighter they stand. At low butanol coverage the molecules are able to lie flatter

to the surface due to the low concentration. Looking at the 72 and 98 butanol coverage, the

average height of the butanol is significantly less than that of the 50 coverage. Also, there are

more butanol molecules with negative values, and that the negative values become very large.

This indicates that the butanol molecules form a bilayer after the 50 butanol coverage. This would also indicate as to why there are such large negative values for the length of the butanol.

Figure 2: A Butanol Bilayer
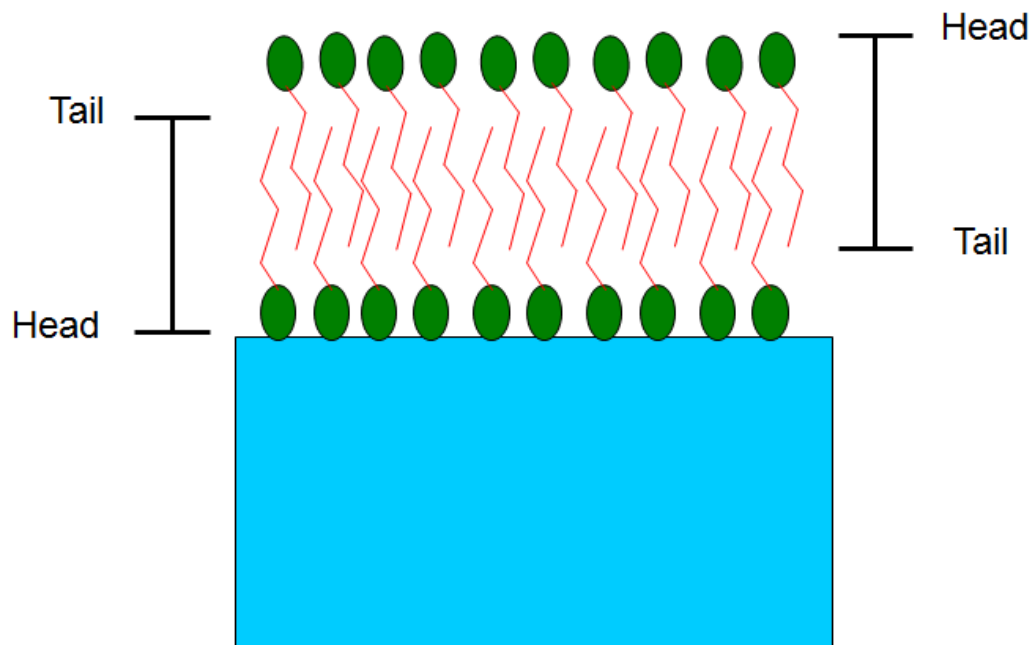
Since the bilayer has polar heads that are now sticking out into the gas phase, it is conceivable that an incoming water molecule approaching the interface would be attracted to the polar heads of the bilayer and may bind to them, never moving down into the bulk of the liquid. After determining that the bilayer is the reason for the increase in the number of condensations, Lawrence and Gilde analyzed the data again, this time only counting a collision as resulting in a condensation if it reached the bulk liquid. Figure 3 shows condensations that made their way all

the way to the bulk, not just those that did not become trapped in the bilayer. This graph shows

the trend that they have seen with increasing concentrations of butanol surfactant.

Figure 3: Percent Condensation in the Water and Butanol Simulation at Different Coverages of Butanol

Water-Butanol Simulation
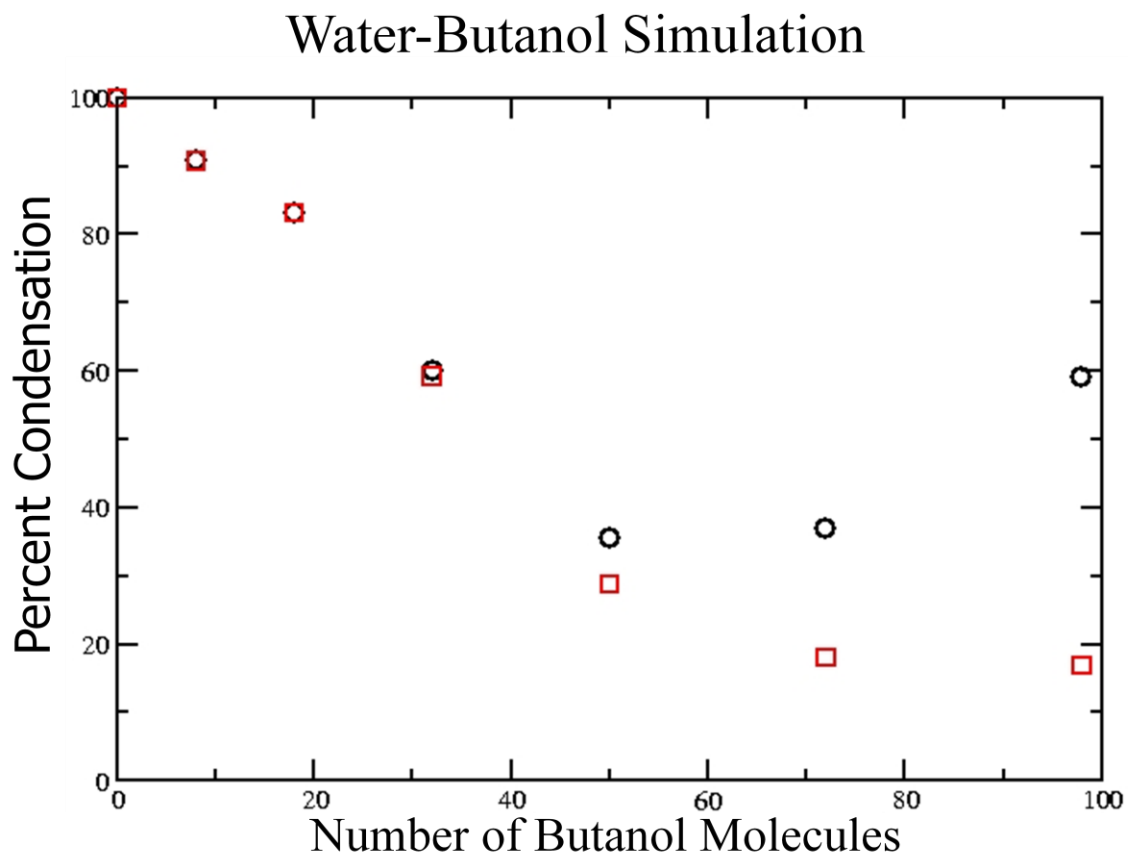
In Figure 3: Percent Condensation in the Water and Butanol Simulation at Different Coverages of Butanol, the black circles show the original percent condensation and the red circles show the new percent condensation which focuses on the molecules that reach the bulk of the liquid.

Looking back at Figure 1, we estimate a complete monolayer of butanol is obtained at 50

butanol, as after this point there is a bilayer forming. Regarding the mechanism of condensation,

they were able to conclude from the simulation that only those molecules that formed a hydrogen bond upon hitting the surface managed to condense.

Comparing the simulation results to the work of Nathanson *et al.* is not possible at this point due to the differences in their systems. Nathanson studied a supercooled sulfuric acid system with a full covering of butanol, while Lawrence and Gilde modeled a system of water with a full covering of butanol at room temperature. To better attempt to model Nathanson's experiment, we have now begun to run our simulations using sulfuric acid in the bulk phase of water.

Methods

To add sulfuric acid to our simulation, we had to determine what concentrations of sulfuric acid solutions we were going to work with. Nathanson had studied three different concentrations, 60, 64, and 68 percent by weight sulfuric acid in water. When sulfuric acid is placed in water, it dissociates into bisulfate and sulfate ions, protonating water into the hydroinum species. Using these three concentrations, we then calculated how many molecules of bisulfate, sulfate, hydronium, and water would be in the system. [17]

The classical molecular dynamics simulations were performed using the SPC/E model for water [18] and the TraPPE-UA force field (a unified atom model) for the alcohols. [19] In addition to the intermolecular interactions described by the SPC/E model, harmonic force constants were employed for internal motion. [20] The parameters for the ionic species (hydronium, sulfate, and bisulfate) were obtained from various sources. [21-23] In all three cases, it was necessary to supplement these models with an intramolecular force field. To do so, we performed electronic structure calculations at the B3LYP/6-311G(d,p) level in which the

bonds and angles were stretched. The results of these calculations were fit to find harmonic

force constants. To find the torsion barrier for rotation of the S-O4 bond, the bond was rotated

within an electronic structure calculation. The barrier was found to be 1.043×10^{-21} J.

Table 2: Force Constants for Hydronium

Atom Pair	Force Constant in Joules / Meters^2
H – O	757.07355
H – H	197.0548

Table 3: Force Constants for Sulfate

Atom Pair	Force Constant in Joules / Meters^2
S-O	595.9676
O-O	238.2084

Figure 3: Numbering Scheme for Bisulfate
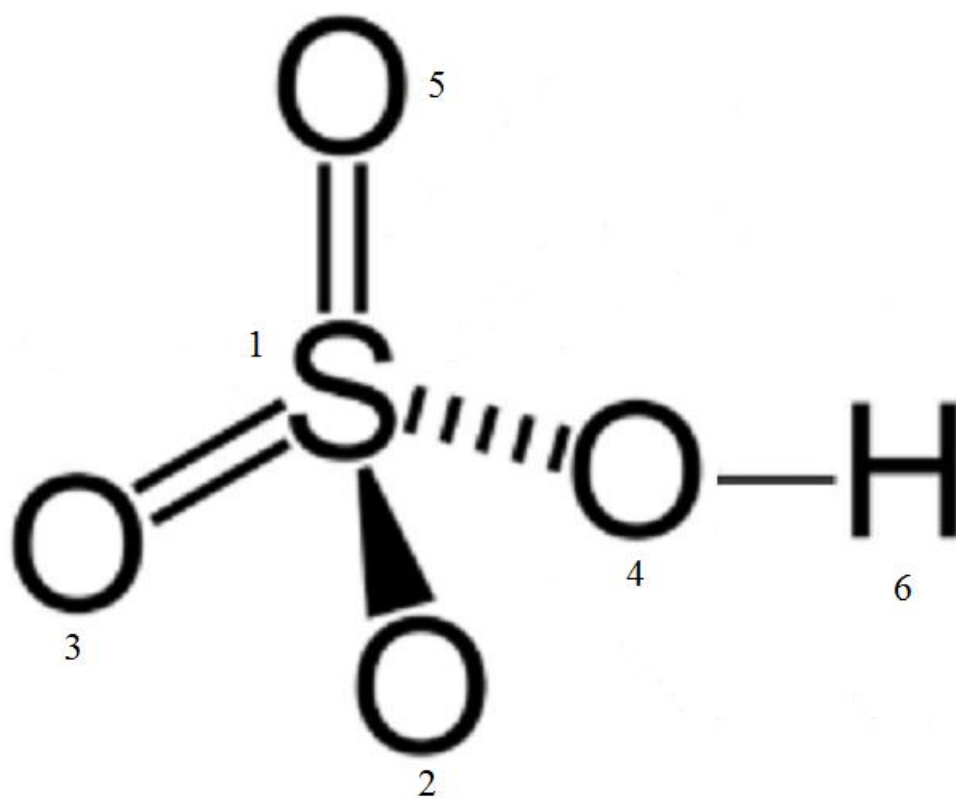
Table 4: Force Constants for Bisulfate

Atom Pair	Force Constant in Joules / Meters^2
1 − 2	845.5501
1 − 3	845.5501
1 − 4	313.7240
1 − 5	845.5501
1 − 6	145.7730
2 − 3	190.4946
2 − 4	194.1632
2 − 5	306.2742
3 − 4	161.0048
3 − 5	188.4823
4 − 5	193.4489
4 − 6	831.4710

Rectangular periodic boundary conditions were applied and the electrostatic forces were calculated using the damped shifted force alternative to the Ewald summation as described by Fennell and Gezelter. [24-26] The damping parameter, alpha, was 0.2 angstroms to the negative one and the cutoff radius was set to 12.3 angstroms (half of the shortest of the box lengths). The equations of motion were integrated using the leapfrog algorithm with a time step of 0.5 fs. In all

cases, the temperature was held constant through velocity scaling at each step. Initially a cubic system containing 500 water molecules was prepared in which the box length was chosen such that the density of the system would be equal to experimental value at 300 K. Velocities were randomly assigned to each atom. The system was equilibrated for 250 ps.

To prepare the sulfuric acid interface, the length of the box was extended in one dimension (z) to 110 angstroms (about four times the length in the original cubic box). To allow the system to reequilibrate after this change, an additional run of 250 ps was performed. For the water/surfactant systems, when the original cubic box was extended, a layer of evenly spaced alcohol molecules was added to the upper and lower interfaces followed by an equilibration run of 250 ps. Simulations were run with surfactant coverage's of 8, 18, 32, 50, 72, and 98 molecules.

After the interfaces were prepared, the scattering simulations were performed by introducing water molecules in the vapor region of the system. The velocities of these molecules were selected based on the Boltzmann distribution for the translational, rotational, and vibrational degrees of freedom. The bonds were also randomly displaced from equilibrium in the same manner. [27] Each molecule was randomly placed in the x and y dimensions and positioned about 10 angstroms from the interface along the z-axis. When the velocity in that direction was assigned to be positive, the molecule approached the lower interface and when the z velocity was negative, the molecule approached the upper interface. Once this molecule had collided with another (defined by an oxygen-oxygen or oxygen-carbon distance of less than 4 angstroms), the simulation continued for an additional 10 ps. At this point, we would return to the original equilibrated interface and insert another vapor molecule. For each system, 250 scattering trajectories were calculated.

Results and Discussion

From these scattering calculations for the three different concentrations of sulfuric acid,

we obtained the following data for the condensation percentage.

Table 5: Percent Condensations at Different Concentrations of Sulfuric Acid and Water

Through Various Butanol Surfactant Coverages

Surfactant Butanol Molecules	Water	60wt%	64wt%	68wt%
8	91%	93%	96%	95%
18	83%	86%	86%	89%
32	59%	64%	77%	72%
50	28%	51%	56%	31%
72	18%	21%	27%	13%

Table 5 shows the results obtained from the 250 runs of the simulation. Nathanson's

experiment was conducted with a full monolayer of butanol molecules, thus we will be looking

at the 50 butanol coverage as this is where a full monolayer of butanol molecules occurs in our

simulations. Focusing on the 50 butanol coverage, the percent condensation is 51 for the 60 wt%

sulfuric acid, 56 for the 64 wt% sulfuric acid, and 30 for the 68 wt% sulfuric acid. The average

percent condensations at the 50 butanol coverage of the acid simulations are significantly higher

than the 28 % obtained from the water butanol simulation. The value of 30 % for the 68 wt% was

not double checked and we hypothesize that the percent is actually higher than that based on the

fact that the rest of the percent condensations do not depend on the acid concentration.

Nathanson's experimentally determined value for the rate of evaporation of sulfuric acid

through a complete monolayer of butanol is about 100% of the rate of evaporation of a bare

sulfuric acid system. Our preliminary results obtained by the sulfuric acid simulations are closer

to the experimental value; however, they are still a factor of 2 less.

After having determined that the condensation percentages were not dependent on the

concentrations of the sulfuric acid systems, we turned towards the idea of a temperature

dependency. However, after obtaining nearly the same percentages at 300K as were obtained at

213K, we were not sure what other cause there might be. We were working toward an

understanding of this difference when we uncovered an error in some of the parameters used for

the sulfuric acid simulations. We have since corrected the errors and are currently running the

new simulations.

Conclusion

Preliminary results of the sulfuric acid simulation indicate that the condensation rate

increases when comparing to the rate obtained by the butanol water simulation. Those

simulations indicated that the change is not a temperature dependant effect, and as such we are

unclear in what is causing the change. Next we plan to rerun the sulfuric acid simulations with

the corrected input values in the program and plan to check if the previous conclusions still hold,

and if so, we plan to work towards understanding why there is a change between the two simulations.

(1) Chuang, P. Y.; Charlson, R. J.; Seinfeld, J. H. *Nature* **1997,** *390,* 594.

(2) Hudson, J. G.; Yum, S. S. *J. Geophys. Res* **1997,** *54,* 2642.

(3) Yum, S. S.; Hudson, J. G.; Xie, Y. *J. Geophys.* Res*,* **1998,** *103,* 16625.

(4) Nenes, A.; Ghan, S.; Abdul-Razak, H.; Chuang, P. Y.; Seinfeld, J. H. *Tellus B.* **2001,** *53,* 133.

(5) Charlson, R. J.; Schwartz, S. E.; Hales, J. M.; Cess, R. D.; J. A. Coakley, J, J.; Hansen, J. E.; Hoffman, D. J. *Science* **1992,** *255,* 423.

(6) Watson, R. T., et al.., Eds. *Intergovernmental Panel on Climate Change, Climate Change 2001: The Scientific Basis;* Cambridge University Press: Cambridge, U. K., 2001.

(7) Rosenfeld, D. *Science* **2000,** *287,* 1793.

(8) Murphy, D. M.; Thomson, D. S.; Mahoney, T. M. *Science* **1998,** *282,* 1664.

(9) Russell, L. M.; Maria, S. F.; Myneni, S. C. B. *Geophys. Res. Lett.* **2002,** *29,*1779.

(10)   Tervahattu, H.; Juhanoja, J.; Kupiainen, K. J. *Geophys. Res. Atmos.* **2002,** *107,* 4319

(11)   Tervahattu, H.; Juhanoja, J.; Vaida, V.; Tuck, A. F.; Niemi, J. V.; Kupiainen, K.; Kulmala, M.; Vehkamaki, H. *J. Geophys. Res. Atmos.* **2005,** *110,* D06207.

(12)   Mer, V. K. L.; Healty, T. W.; Aylmore, L. A. G. *J. Colloid Sci.***1964,** *19,* 673.

(13)   Barnes, G. T. *Colloids Surf. A* **1997,** *126,* 149.

(14)	Lawrence, J. R.; Glass, S. V.; Nathanson, G. M. *J. Phys. Chem. A* **2005,** *109,* 7449.

(15)	Lund Myhre, C. E.; Christensen, D. H.; Nicolaisen, F. M.; Nielsen, C. J. *J. Phys. Chem. A,* **2003,** *107,* 1979.

(16)	Gilde, A.; Siladke, N.; Lawrence, C. P., *J. Phys. Chem. A* **2009,** *113,* 8586.

(17)	Morita, A.; Sugiyama, M.; Kameda, H.; Koda, S.; Hanson, D. R. *J. Phys. Chem. B* **2004,** *108,* 9111.

(18)	Berendsen, H. J. C.; Grigera, J. R.; Straatsma, T. P. *J. Phys. Chem.* **1987,** *91,* 6269

(19)	 Chen, B.; Potoff J. J.; Siepmann, J. I., *J. Phys. Chem. B* **2001,** *105,* 3093

(20)	Toukan, K.; Rahman, A. *Phys. Rev. B* **1985,** *31,* 2643.

(21) Rodwell, W. R.; Radom, L., *J. Am. Chem. Soc.* **1981,** *103,* 2865.

(22) Lau, K.Y.; Ikuta, S.; Kebarle, P., *J. Am. Chem. Soc.* **1982,** *104,* 1462.

(23) Kuasaka, I.; Wang, Z.-G.; Seinfeld, J.H., *J. Chem. Phys.* **1998,** *108,* 6829.

(24) Fennel, C. J.; Gezelter, J. D. *J. Chem. Phys.* **2006,** *124,* 234104.

(25) Wolf, D.; Keblinski, P.; Phillpot, S. R.; Eggebrecht, *J. Chem. Phys.* **1999,** *110,* 8254.

(26) Zahn, D.; Schilling, B.; Kast, S. M. *J. Phys. Chem. B* **2002,** *106,* 10725.

(27) McQuarrie, D. A. *Statistical Mechanics;* Harper and Row: New York, 1976.